Available online at www.sciencedirect.com
ScienceDirect
Bioorganic & Medicinal Chemistry Letters 18 (2008) 576–585
Bioorganic & Medicinal Chemistry Letters

From rigid cyclic templates to conformationally stabilized acyclic scaffolds. Part I: The discovery of CCR3 antagonist development candidate BMS-639623 with picomolar inhibition potency against eosinophil chemotaxis☆

Joseph B. Santella, III, Daniel S. Gardner, Wenqing Yao, Chongsheng Shi, Prabhakar Reddy, Andrew J. Tebben, George V. DeLucca, Dean A. Wacker, Paul S. Watson, Patricia K. Welch, Eric A. Wadman, Paul Davies, Kimberly A. Solomon, Dani M. Graden, Swamy Yeleswaram, Sandhya Mandlekar, Ilona Kariv, Carl P. Decicco, Soo S. Ko, Percy H. Carter and John V. Duncia*

Bristol-Myers Squibb Company, R&D, PO Box 4000, Princeton, NJ 08543-4000, USA

Received 20 July 2007; revised 16 November 2007; accepted 19 November 2007
Available online 22 November 2007

Abstract—Conformational analysis of *trans*-1,2-disubstituted cyclohexane CCR3 antagonist **2** revealed that the cyclohexane linker could be replaced by an acyclic *syn*-α-methyl-β-hydroxypropyl linker. Synthesis and biological evaluation of mono- and disubstituted propyl linkers support this conformational correlation. It was also found that the α-methyl group to the urea lowered protein binding and that the β-hydroxyl group lowered affinity for CYP2D6. Ab initio calculations show that the α-methyl group governs the spatial orientation of three key functionalities within the molecule. α-Methyl-β-hydroxypropyl urea **31** with a chemotaxis IC_{50} = 38 pM for eosinophils was chosen to enter clinical development for the treatment of asthma.

Eotaxin[1a] is a chemotactic cytokine which binds to CCR3 (CC chemokine receptor 3), the dominant functional chemokine receptor found on eosinophils. It is believed that eotaxin, secreted by bronchial epithelial/endothelial cells, triggers eosinophils to migrate into the lungs of allergic asthmatic patients. Once there, the eosinophils release major basic protein, membrane-derived lipid mediators, proteins, and other toxic substances. The result is bronchial mucosal damage which is thought to give rise to the clinical features of asthma–airway obstruction and bronchial hyperresponsiveness (for a more detailed etiology, see Supplementary material, Figure 1, electronic edition). Thus, a small molecule antagonist of the CCR3 receptor might be an effective drug for the treatment of asthma.[1b]

We have previously described the discovery of acyclic[2] and cyclic[3] CCR3 antagonists **1** and **2**, respectively, both of which exhibit nanomolar binding potency[4] as shown in Table 1. While the potency of both classes of inhibitors, as measured by the binding inhibition, levels out at 1 nM, the potency as measured by chemotaxis inhibition can be in the double-digit picomolar range.[5] Thus, we see that cyclohexyl-containing compounds **2b** and **2a** are 300- and 700-fold more potent inhibitors of eosinophil chemotaxis than are **1b** and **1a**, respectively, even though they all have about the same binding IC_{50} value of 1–2 nM.[5]

We hypothesized that the superior chemotaxis inhibition potency of cyclic inhibitor **2** relative to the acyclic **1** stems from the conformational rigidity of the *trans*-

Keywords: CCR3 antagonist; BMS-639623; Development candidate; Ab initio; Eosinophil chemotaxis; Asthma; Conformational analysis; Acyclic scaffold.

☆ This work was originally presented by J.V.D. at *Balticum Organicum Syntheticum 2004*, *BOS2004*, a biennial international conference on organic synthesis, June 23, 2004, Riga, Latvia: www.BOS06.ttu.ee and link to 2004 abstracts.

* Corresponding author. Tel.: +1 609 252 3123; e-mail: john.duncia@bms.com

0960-894X/$ - see front matter © 2007 Elsevier Ltd. All rights reserved.
doi:10.1016/j.bmcl.2007.11.067

Table 1. Binding and chemotaxis IC_{50} values for compounds **1** and **2**

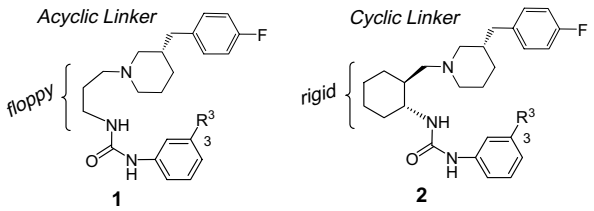

Compound	R^3	CCR3 IC_{50}[a,b] (nM)	Chemotaxis IC_{50}[a,b] (nM)	CYP2D6 IC_{50}[a] (μM)	PB % free
1a	Ac	2.5 ± 1.2	25	0.5	—
1b	Tet[c]	0.6 ± 0.4	3.2 ± 1.6	1.6 ± 0.7	0.6 ± 0.6
2a	Ac	2.0 ± 0.7	0.034 ± 0.019	0.06	—
2b	Tet	1.0 ± 0.5	0.010 ± 0.010	0.2	6.6 ± 1.5

[a] See Ref. 3 for binding and chemotaxis assays.
[b] Values without standard deviations represent a single determination.
[c] Tet = 1-methyl-tetrazol-5-yl.

1,2-disubstituted cyclohexane ring. To test this hypothesis, we sought to rigidify **1** by introducing substituents on the propyl linker to favor only a few low energy conformations. Conformational analysis of the cyclohexane ring dictates the diequatorial placement of the substituents as shown in Newman projection **3** (Fig. 2). Dissection of the ring of **2** leads to an α,β-disubstituted propyl-containing compound, existing in the three low energy conformers, **4**, **5**, and **6**. Conformer **4** is of lowest energy and thus most favored since it only has two gauche interactions instead of three as in conformers **5** and **6**. Conformer **4** also mimics the 60° relationship between the CH_2-piperidine and the urea which is found in the cyclohexyl template of **2**. We assume this 60° relationship is critical for potency. Redrawing Newman projection **4** yields *syn*-disubstituted propylurea **7**. In this very naïve analysis we assumed that there were no other interactions besides the nonbonding gauche interactions. If the piperidine nitrogen is not protonated in the receptor, then H-bonding might occur between the piperidine nitrogen and one of the urea nitrogens to form a six-membered ring. This intramolecular H-bonding can take place only in conformers **4** and **6** and not in **5**. Thus conformer **4** is again the most favored for having both the least number of gauche interactions and for potentially having a stabilizing intramolecular H-bond.

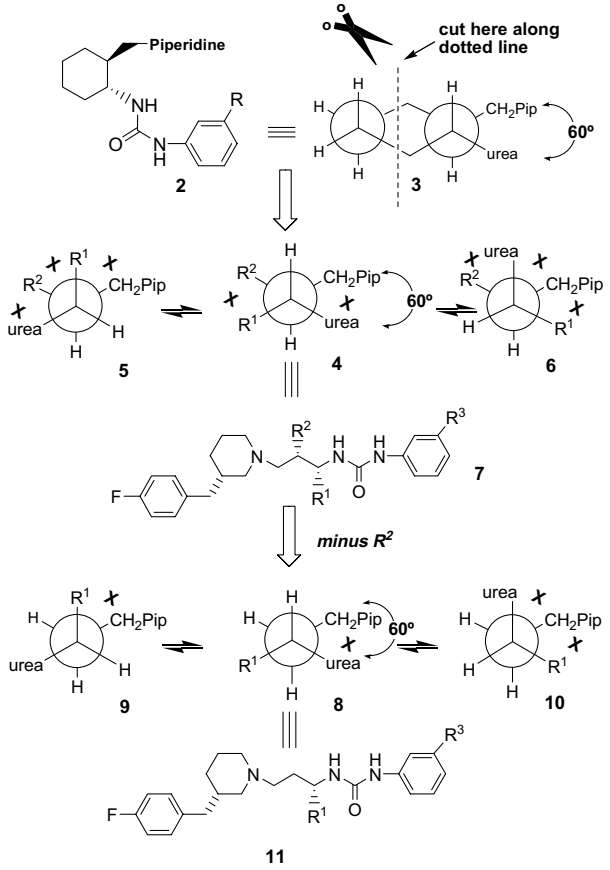

Figure 2. Conformational analysis of compound **2** leading to structures **7** and **11**. '**X**' denotes unfavorable gauche interactions.

What effect would only one substituent have on the number of low energy conformers? This would simplify our target since there would be only one chiral center on the propyl linker instead of two. Substitution of R^2 = H in **4** or **7** (Fig. 2) leads to structure **8** or **11**, respectively. For this monosubstituted propyl linker, there are two low energy conformers, **8** and **9**, when only nonbonding gauche interactions are considered. Of the two, only conformer **8** mimics the 60° relationship between the CH_2-piperidine and the urea. Being in the right conformation part of the time should make the monosubstituted linker slightly less potent than the disubstituted linker where only the correct conformer **4** is preferred. However, potentially intramolecular H-bonding can take place between the piperidine nitrogen and the urea in conformer **8**, but not in **9**. Thus as was the case for the disubstituted linker, a single conformer **8** is favored when only one R^1 substituent is present.

We were extremely delighted to find that the addition of a simple methyl group α to the urea increases the chemotaxis inhibition potency anywhere from 3-fold (**12** vs **1b**) to 50-fold (**26** vs **25**) (Table 2). Unfortunately, the

Table 2. α-Methyl-substituted CCR3 antagonists and their CCR3 binding, chemotaxis, CYP2D6 inhibition, and PB activities

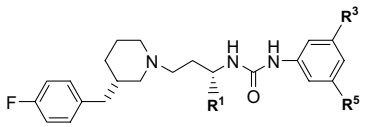

Compound	R^1	R^3	R^5	Binding IC_{50}[a,b] (nM)	Chemotaxis IC_{50}[a,b] (nM)	CYP2D6 IC_{50}[b] (μM)	PB % free
1b	H	H	Tet[c]	0.6 ± 0.4	3.2 ± 1.6	1.6 ± 0.7	0.6 ± 0.6
12	Me	H	Tet	1.3 ± 0.3	1.1	0.4	11
13	H	Me	Tet	1.5 ± 1.0	1.0 ± 0.4	14	0
14	Me	Me	Tet	1.2 ± 0.4	<0.03	0.2	8
15	H	Et	Tet	1.0 ± 0.3	—	1.3	—
16	Me	Et	Tet	2.0 ± 1.3	0.02 ± 0.01	0.8	4
17	H	*i*-Pr	Tet	2.6 ± 0.6	0.30	4.6	0
18	Me	*i*-Pr	Tet	2.6 ± 0.4	0.021 ± 0.02	1.6	2
19	H	$(CH3)_2COH$	Tet	1.1 ± 0.2	0.304	22	15
20	Me	$(CH3)_2COH$	Tet	0.7 ± 0.4	<0.100	17	—
21	H	Ac	Ac	1.2 ± 0.4	3	2.2	0
22	Me	Ac	Ac	2.7 ± 0.8	0.2 ± 0.03	1.3	4
23	H	Ac	Tet	2.6 ± 1.4	—	37.7	—
24	Me	Ac	Tet	1.5 ± 0.2	0.02 ± 0.1	2.1 ± 0.3	13
25	H	Pyraz[c]	Pyraz	1.6 ± 0.8	5	2.8	1
26	Me	Pyraz	Pyraz	1.7 ± 1.0	0.1	3.0	1

[a] See Ref. 3 for binding and chemotaxis assays.
[b] Values without standard deviations represent a single determination.
[c] Tet = 1-methyltetrazol-5-yl; pyraz = pyrazol-1-yl.

methyl group mimics the cyclohexyl template somewhat since it also seems to slightly increase binding to cytochrome P450 CYP2D6, a problem often encountered in the cyclohexyl series (Table 1, compounds **2a**, **2b**). Protein binding had been a problem in the unsubstituted acyclic series. However, we now find that serum protein binding decreases, with % free fraction going from 0.6% for **1b** to 11% free for its α-methyl analog **12**. We had hypothesized that this α-methyl group would disrupt H-bonding between the urea and serum protein. We see increases in free fraction for other compound couplets as well, albeit smaller. For the bispyrazoles **25** and **26**, however, it remains the same at 1%. *Meta*-substitution proved optimal on the phenylurea (SAR not shown). 3,5-Disubstitution (dubbed as the '3,5-effect') further increases chemotaxis inhibition potency up to 50-fold (compare **14**, **16**, **18**, **20**, **24** with **12**). Both of these trends were also seen in the unsubstituted propyl linker series.[2] These aryl substituents most likely bind to two different receptor subsites effectively locking the phenylurea in place. None of the compounds in Table 2 were advanced due to selectivity problems with binding to CYP2D6 or other 7TM receptors, high protein binding, or poor PK (data not shown).

What happens if the α-methyl is enlarged? With longer α-alkyl substituents, the chemotaxis IC_{50} seems to become even more potent (Table 3). However, this increase in potency is at the expense of increased CYP2D6 binding. Longer alkyl substituents also exhibit decreased metabolic stability in human liver microsomes (projected human clearance[6]) possibly due to the greater number of alkyl positions which can be oxidatively metabolized by CYPs.

Before we embarked on making disubstituted propyl linkers, we needed to know in the monosubstituted series if we were working with the more potent linker enantiomer, since one was more potent than the other in the cyclic series.[3] In Table 4 when X = H_2, there is a 2- and a 3-fold difference in binding potencies in the isomeric pairs of piperidines **22/22a** and **12/12a**. However, the difference in chemotaxis IC_{50} values for isomers **22/22a** is 300-fold! In the more rigid X = O molecules, the difference in binding potencies in the isomeric pair of piperidineamides **29/29a** is even more pronounced. Piperidineamides, such as **29**, were not pursued any further because of undetectable free compound in blood serum. Compounds **29/29a**, in which there is no basic nitrogen, display lower affinity for CYP2D6 compared to their counterparts **12/12a**.

As discussed earlier, disubstituted propyl linkers **7** should be more potent than monosubstituted **11** when only nonbonding gauche interactions are considered in the conformational analysis (i.e., no intramolecular H-bonding). Thus, we embarked to see what effect $R^2 \neq H$ would have on potency. We chose $R^2 = OH$ since it could easily be introduced (see Chemistry) while at the same time it would decrease lipophilicity and thus possibly CYP2D6 binding. We find that adding $R^2 = OH$ to the propyl linker does increase chemotaxis inhibition potency as seen when comparing compounds **12** and **31** (27-fold, Table 5), both of which contain a monosubstituted phenylurea. However, for the other cases, all of which contain the potency-enhancing 3,5-disubstituted phenylurea, the chemotaxis inhibition potency remains about the same. Apparently, the '3,5-effect' maximizes potency to such an extent that an

Table 3. α-Alkyl-substituted CCR3 antagonists and their CCR3 binding, chemotaxis, and CYP2D6 IC_{50} values together with projected human clearance

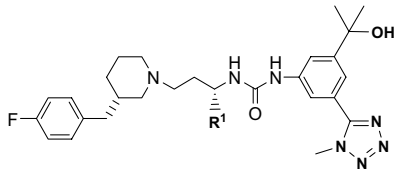

Compound	R^1	Binding IC_{50}[a,b] (nM)	Chemotaxis IC_{50}[a,b] (nM)	CYP2D6 IC_{50}[b] (μM)	CL (projected human clearance)[6] mL/min/kg
19	H	1.1 ± 0.2	0.3	22	12
20	Me	0.7 ± 0.4	<0.1	17	12
27	Et	2.4 ± 0.2	0.1	8.2	15
28	*n*-Pr	1.5 ± 0.6	0.011	1.0	17

[a] See Ref. 3 for binding and chemotaxis assays.
[b] Values without standard deviations represent a single determination.

Table 4. Enantiomeric pairs of CCR3 antagonists with their binding, chemotaxis, and CYP2D6 activities

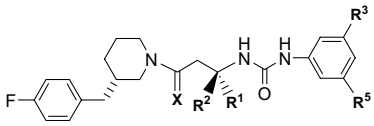

Compound	X	R^1	R^2	R^3	R^5	Binding IC_{50}[a,b] (nM)	Chemotaxis IC_{50}[a,b] (nM)	CYP2D6 IC_{50}[b] (μM)
22	H_2	Me	H	Ac	Ac	2.7 ± 0.8	0.2 ± 0.03	1.3
22a	H_2	H	Me	Ac	Ac	5.8 ± 1.1	60	3.5
12	H_2	Me	H	H	Tet[c]	1.3 ± 0.3	1.1	0.4
12a	H_2	H	Me	H	Tet	4.0 ± 0.7	>1	0.2
29	O	Me	H	H	Tet	4.2 ± 1.2	0.2	4.4
29a	O	H	Me	H	Tet	37% at 0.3 μM	—	>100

[a] See Ref. 3 for binding and chemotaxis assays.
[b] Values without standard deviations represent a single determination.
[c] Tet = 1-methyltetrazol-5-yl.

additional R^2 = OH group has little or no effect on chemotaxis inhibition (compare **22** and **30**, **14** and **34**, **16** and **35**, **18** and **36**, **26** and **37**). The other possibility is that chemotaxis inhibition potency is completely in line with our earlier prediction that both the monosubstituted (i.e., **11**) and disubstituted (i.e., **7**) linkers should be equipotent when intramolecular H-bonding interactions are invoked. Thus couplet **12** and **31** would be the only exception. This would mean that in compound **12**, intramolecular H-bonding does not occur for some odd reason, since it is much less potent than its 3,5-disubstituted counterparts **14**, **16**, and **18**. There is nothing radically different structurally in compound **12** from the other more potent monosubstituted linker compounds to prevent intramolecular H-bonding. Thus the first explanation seems to be more accurate: the potency differences amongst the monosubstituted linkers arise from the presence or absence of 3,5-disubstitution on the phenylurea while intramolecular H-bonding between the urea and piperidine is very minimal to nonexistent. Thus in summary, introduction of a β-substituent such as R^2 = OH increases potency unless the 3,5-disubstituted phenylurea is present.

The addition of a polar R^2 = OH group to our delight always weakened CYP2D6 binding affinity as seen in the following compound comparisons: **22** and **30** (5-fold), **12** and **31** (6-fold), **32** and **33** (6-fold), **14** and **34** (17-fold), **16** and **35** (3-fold), **18** and **36** (3-fold), **26** and **37** (2-fold), **40** and **41** (2-fold). We also observe the same order of increasing potency for CYP2D6 with increasing size of the R^1 substituent: **45** > **44** > **31**. Protein binding either becomes slightly better or stays about the same with the addition of a R^2 = OH group. The linker enantiomer of **30** was synthesized where both R^1 and R^2 are *syn* and β (**30a**) to doublecheck whether we were still working with the more potent diastereomer. We find that **30** is more potent than **30a** in both binding (3-fold) and chemotaxis inhibition (>17-fold).

A wide variety of R^2 groups are tolerated and yield potent compounds. However, none could be advanced except for R^2 = OH. For example, carbamate derivatives of the OH group, such as **48**, are all potent, but suffer from instability in human liver microsomes. Replacement of R^2 with an amino group leads to dibasic molecule **49** which exhibits potent CYP2D6 inhibition. Acetamide **50** exhibits poor oral absorption in the mouse. Dimethylamino analog **51** is unstable to human liver microsomes, most likely due to *N*-demethylation. Finally, the α,β-dimethyl analog **52** (which is a direct mimic of **2b** except for two carbons missing from the cyclohexyl ring) has good potency, but it is extremely unstable in human liver microsomes with a high intrinsic clearance value of 20.0 mL/min/kg.

Table 5. α-Methyl-β-hydroxy-substituted CCR3 antagonists **7** and their CCR3 binding, chemotaxis, CYP2D6 inhibition, and PB activities[a]

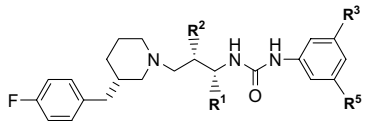

7

Compound	R^1	R^2	R^3	R^5	Bind. IC_{50}[a,b] (nM)	Chemotaxis IC_{50}[a,b] (nM)	CYP-2D6 IC_{50}[b] (μM)	PB % free
21	H	H	Ac	Ac	1.2 ± 0.4	3	2.2	0
22	Me	H	Ac	Ac	2.7 ± 0.8	0.2 ± 0.03	1.3	4
30	Me	OH	Ac	Ac	0.8 ± 0.3	0.06 ± 0.05	7.0	4
30a	Me[d]	OH[d]	Ac	Ac	2.7 ± 1.4	>1	16	—
1b	H	H	H	Tet[c]	0.6± 0.4	3.2 ± 1.6	1.6 ± 0.7	1
12	Me	H	H	Tet	1.3 ± 0.3	1.1	0.4	11
31	Me	OH	H	Tet	0.3 ± 0.03	0.04 ± 0.01	2.6	16
32	Me	H	Br	Tet	1.7 ± 0.3	—	0.5	0
33	Me	OH	Br	Tet	1.8 ± 0.7	0.05	3.1	0
14	Me	H	Me	Tet	1.2 ± 0.4	<0.03	0.2	8
34	Me	OH	Me	Tet	0.5	<0.03	3.5	8
16	Me	H	Et	Tet	2.0 ± 1.3	0.02 ± 0.01	0.8	4
35	Me	OH	Et	Tet	1.8 ± 0.6	0.013	2.5	5
18	Me	H	*i*-Pr	Tet	2.6 ± 0.4	0.02 ± 0.02	1.6	2
36	Me	OH	*i*-Pr	Tet	1.0 ± 0.6	0.02 ± 0.01	4.7	5
26	Me	H	Pyraz[c]	Pyraz	1.7 ± 1.0	0.1	3.0	1
37	Me	OH	Pyraz	Pyraz	2.6	0.05	5.9	2
38	Me	OH	H	Imid	0.3	1.0	3.3	—
39	Me	OH	Thiaz[c]	Thiaz	0.8	—	0.8	—
40	Me	H	Triaz[c]	Triaz	2.0 ± 0.6	—	0.5	—
41	Me	OH	Triaz	Triaz	1.4 ± 0.7	—	0.9	—
42	Me	OH	Oxaz[c]	Oxaz	2.7 ± 1.2	—	0.5	—
43	Me	OH	Isox[c]	Isox	1.1 ± 0.6	0.1	1.5	—
44	Et	OH	H	Tet	1.0 ± 0.2	—	0.9	—
45	*n*-Pr	OH	H	Tet	0.6 ± 0.2	—	0.5	—
46	*i*-Pr	OH	H	Tet	0.4[c]	—	0.3	—
47	*i*-Bu	OH	H	Tet	1.2 ± 0.4	—	0.6	—
48	Me	OCONHMe	H	Tet	0.5 ± 0.1	0.87	4.0	—
49	Me	NH2	H	Tet	1.2 ± 0.6	—	0.4 ± 0.2	—
50	Me	NHAc	H	Tet	0.6 ± 0.2	—	3.8	—
51	Me	NMe_2	Et	Tet	0.5[c]	<0.03	1.4	—
52	Me	Me	H	Tet	1.8 ± 0.2	0.064	2.2	6

[a] See Ref. 3 for binding and chemotaxis assays.
[b] Values without standard deviations represent a single determination.
[c] See Ref. 7 Tet = 1-methyltetrazol-5-yl; pyraz = pyrazol-1-yl; imid = 1-methylimidazol-2-yl; thiaz = thiazol-2-yl; triaz = triazol-1-yl; oxaz = oxazol-2-yl; isox = isoxazol-3-yl.
[d] R^1 and R^2 are both *syn* and β and constitute the enantiomeric linker of **30**.

Table 6. Oral bioavailability of BMS-639623 (**31**) in the mouse, rat, dog, cyno, and chimp

Species	Dose mg/kg po	% *F*	C_{max} (nM)	AUC (nM h)
Mouse	10	57	1542	3151
Rat	50	45	3170	21341
Dog	10	17	926	2740
Cyno	10	19	561	1055
Chimp	2	16	173	639

Based on its excellent potency, weak CYP2D6 inhibition, and reasonable free fraction, compound **31** (BMS-639623) was selected for further evaluation. It was orally bioavailable in five species (Table 6) as well as selective against other 7TM receptors and ion channels. In addition to human eosinophil chemotaxis inhibition, **31** also showed activity in another functional assay, namely eotaxin-stimulated calcium flux in eosinophils[4] where it exhibited an IC_{50} of 0.87 nM (±0.41 ($n = 6$)). Because **31** has poor binding and chemotaxis inhibition potency in the mouse (IC_{50} = 31, 870 nM, respectively), it was dosed intranasally in a *Ascaris suum* challenge model in the cyno (cyno eosinophil chemotaxis IC_{50} = 0.15 nM). The cyno study was a cross-over design in which five animals were dosed orally with either vehicle or **31** at 5 mg/kg b.i.d. at 2 h before and 10 h after *A. suum* aerosol challenge. Twenty-four hours after challenge, the animals underwent bronchoalveolar lavage and the eosinophil number was determined. In three animals, **31** reduced the allergen-dependent eosinophilia by 65%, 78%, and 82% while in two animals there was no response. Trough plasma levels of the compound in all animals were at or above the theoretical total concentrations required to inhibit in vitro cyno eosinophil chemotaxis at the IC_{90} (5 nM) levels. After passing preclinical toxicology and cardiovascular assessment, compound **31** was nominated for clinical development.

Computer modeling. Further support to our conformational correlation between the cyclohexyl template and the mono- and disubstituted propyl linkers comes from ab initio calculations[8a] done on the four model systems shown in Figure 3. We find that as previously predicted, the α-methyl-β-hydroxypropyl linker (model 4) and the α-methylpropyl linker (model 3) share the same lowest energy conformation about bond #1 ($\phi = -60$, Fig. 3; conformation **4**, or **8**, Fig. 2) and mimic the cyclohexyl template's lowest energy conformation (model 1, $\phi = -60$, Fig. 3; conformation **3**, Fig. 2). The lowest energy conformers of the substituted acyclic linkers are favored over the other two conformers by 1–2 kcal/mol.

What the ab initio calculations further show is that the α-methyl group mimics the cyclohexyl's influence on the conformation about bond #2, the α-carbon–urea bond. In Figure 4 we see that the lowest energy conformer is the same amongst models 1, 3, and 4 which is favored over the other rotamer by 1–2 kcal/mol. This most favored conformation relieves 1,3-allylic strain if one lends double-bond character to the urea's NH–CO bond.[9] Thus, the influence on conformation by the α-methyl group is profound: not only does it influence the orientation of the piperidine and urea relative to one another via the lowest energy conformer about bond #1, but it also influences the orientation of the urea about bond #2. Given the rigidity of the urea, this in turn influences the spatial orientation of the urea 'tail end', that is, the phenyltetrazole of **31**. *Thus, the spatial orientation of three key functional groups, the piperidine, the urea, and the urea tail piece, is governed by a single methyl group!*

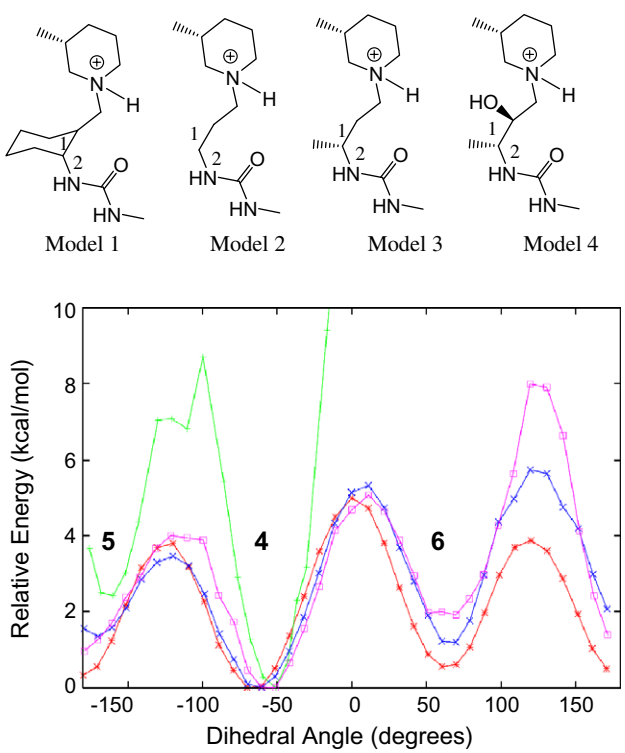

Figure 3. Energetic profile of the central dihedral about bond #1 of the model systems. Model 1 is in green, model 2 in red, model 3 in blue, and model 4 in purple. Energies are reported as relative to the global minimum of each model. Model 1 is only evaluated in the torsional range of −180 to 0 because of the geometrical constraints of the cyclohexyl ring. The inset numbers denote geometries equivalent to the structures shown in Figure 2.

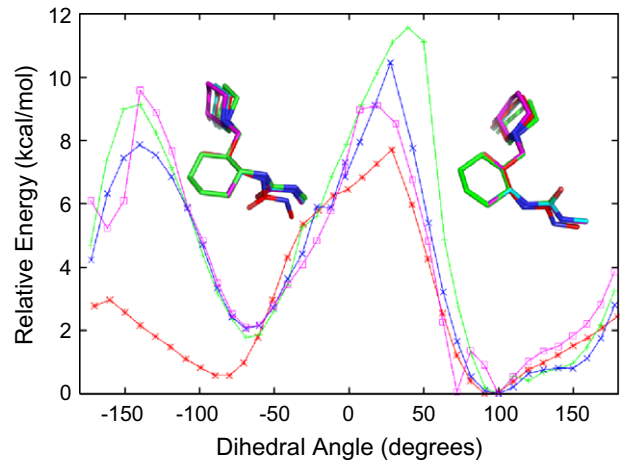

Figure 4. Dihedral drive around the connecting urea C–N bond. Model 1 is in green, model 2 in red, model 3 in blue, and model 4 in purple. The inset structures are an overlay of the lowest energy structures for the corresponding local minimum.

Chemistry. The compounds in Tables 2–5 were synthesized by a slight modification of the method of Davies[10a] as exemplified in Scheme 1. Starting materials **53** and **60** were synthesized as described previously.[3] Upon Michael-type addition of **56**–**55**, the intermediate enololate may be optionally quenched with the chiral Davis[10b] oxaziridine to yield hydroxyl substituted propyl linkers as per the method of Davies.[10a]

A scalable synthesis of the monomethyl substituted propyl linkers starting from L-aspartic acid derivative **62** is shown in Scheme 2. The method of Beaulieu[11] as shown in Scheme 3 was used to make 700 g of **31** starting from D-alanine. Scheme 4 shows the synthesis of **49** and **50** via an adaptation of the method of Davies.[12] Scheme 5 shows a synthesis of **51** starting from a protected D-threonine. The α,β-dimethylpropyl linker of compound **52** was synthesized using the methodology of Davies.[13] Schemes 6–10 describe the synthesis of the key intermediates for the substituted phenylureas in Tables 2, 3 and 5. 3,5-Bis-acetylaniline was synthesized by the method of Ulrich,[14] followed by conversion to phenylurea as in Scheme 6.

Conclusion. We have converted cyclic molecules into acyclic ones via conformational analysis which has yielded molecules exhibiting binding affinities in the single digit nanomolar range. These binding affinities translate into a pharmacological effect, namely the in vitro picomolar inhibition of human eosinophil chemotaxis, the inhibition of eotaxin-induced Ca^{2+} mobilization, and the in vivo inhibition of allergen-induced eosinophilia in the cyno. It remains to be seen whether in human clinical trials, compound **31** will alleviate the symptoms of asthma via the in vivo inhibition of eosinophil chemotaxis. We have also shown that the *syn*-α,β-

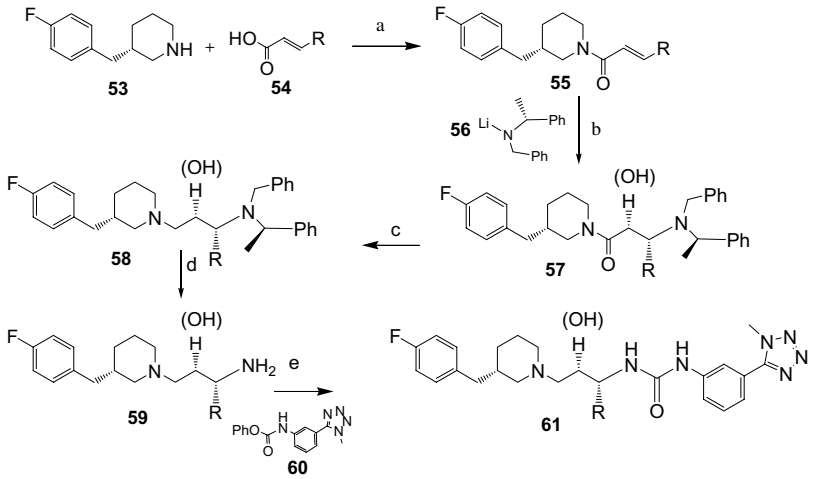

Scheme 1. Reagents and conditions: (a) PyBOP, Et_3N, CH_2Cl_2, rt, 24 h, quant; (b) −78 °C, THF, **56**, followed by optional *S*-(+)-camphor-sulfonyloxaziridine quench to introduce OH group, 53–65%; (c) B_2H_6, THF, rt, 90%; (d) $Pd(OH)_2$, H_2, MeOH, AcOH, rt, 55–93%; (e) **60**, acetonitrile, 25 °C.

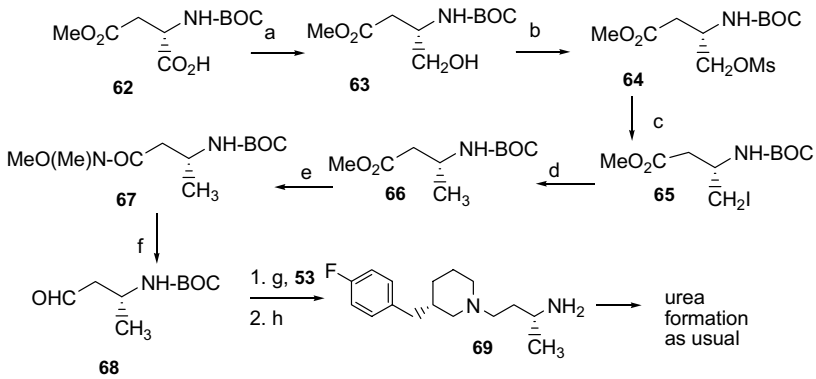

Scheme 2. Reagents and conditions: (a) i—B_2H_6, THF, 0 °C, ii—HOAc, MeOH, 76%; (b) MsCl, Et_3N, Et_2O, rt, 70%; (c) LiI, THF, ultrasound, 92%; (d) $Pd(OH)_2$, H_2, MeOH, quant; (e) i—LiOH, ii—HN(Me)OMe–HCl, BOP, lutidine, 66%; (f) i—DIBAL, −78 °C, ii—acetone, iii—tartaric acid aq 88%; (g) $NaB(OAc)_3H$, 80–90%; (h) TFA, CH_2Cl_2, quant.

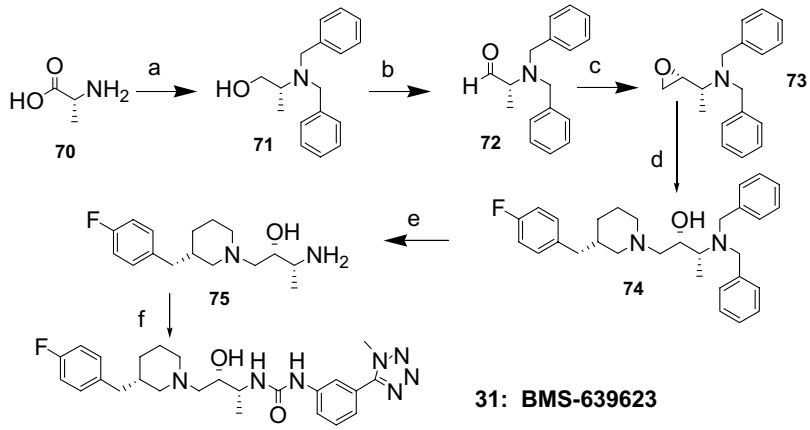

Scheme 3. Reagents and conditions: (a) i—BnBr, K_2CO_3, EtOH, rt; (ii) LAH, reflux, 24 h, 72%; (b) DMSO, Py–SO_3, 10–15 °C, 2 h, 96% crude; (c) CH_2Br_2, THF, *n*-BuLi, −55 °C, 95%, 6:1 mixture of diastereomers; (d) **53**, EtOH, reflux, 20 h, two fractions isolated: 37% of an 8:1 mixture of diastereomers and 36% of a 6:1 mixture of diastereomers; (e) $Pd(OH)_2$, H_2, MeOH, HOAc, 24 h, 82%, 81%, after R-mandelic acid recrystallization; (f) **60**, CH_3CN, rt, 20 h, 86%, HPLC = 98.7%.

disubstituted propyl linker is isosteric with a *trans*-1,2-disubstituted cyclohexane. Ab initio minimized structures of **2b** and **31** are overlapped in Figure 5. The two compounds are conformationally indistinguishable with regard to (1) overlap of the cyclohexyl of **2b** and the *syn*-α-methyl-β-hydroxy-propyl linker of **31**, (2) the

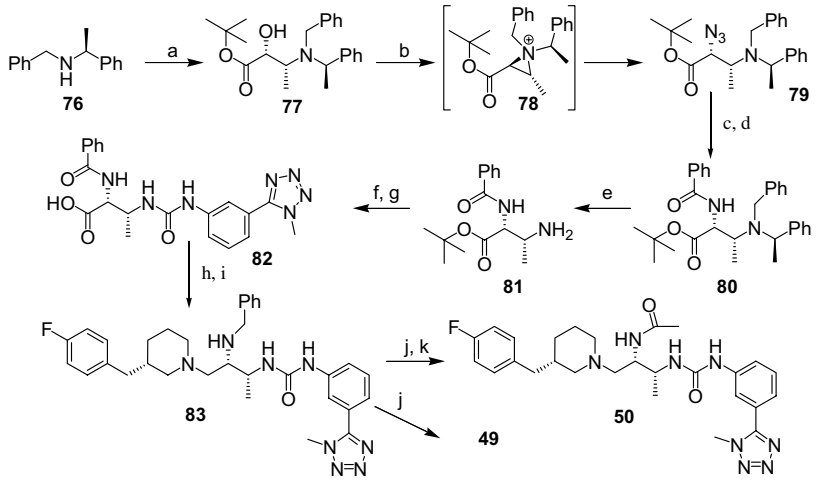

Scheme 4. Reagents and conditions: (a) i—*n*-BuLi; ii—*tert*-Butyl crotonate; iii—*S*-(+)-camphor-sulfonyloxaziridine, THF, 39%; (b) DPPA, DEAD, NaN_3, THF, 90%; (c) H_2, 10% Pd–C, EtOAC/MeOH, 50 psi, 1 h, 90%; (d) Ph(CO)Cl, Et_3N, THF, 93%; (e) H_2, $Pd(OH)_2$, MeOH; (f) **60**, Et_3N, DMF, 66% for steps e and f; (g) TFA, CH_2Cl_2; (h) **53**, PyBop, Et_3N, 20% for steps g and h; (i) B_2H_6, THF, 40%; (j) H_2, $Pd(OH)_2$, MeOH, 50 psi, 69%; (k) Ac_2O, Et_3N, CH_2Cl_2, 98%.

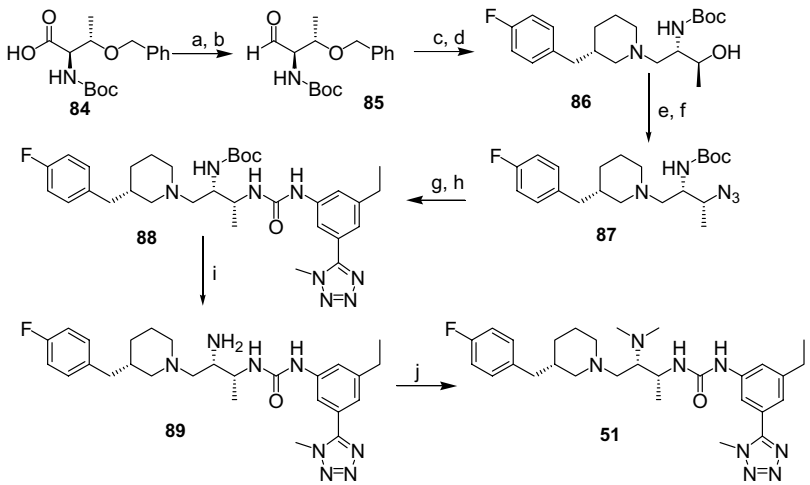

Scheme 5. Reagents and conditions: (a) *N*,*O*-dimethylhydroxylamine hydrochloride, PyBop, Et_3N, 70%; (b) DIBAL-H, CH_2Cl_2, −78 °C, 78%; (c) **53**, $Na(OAc)_3BH$, CH_2Cl_2, 81%; (d) H_2, 10% Pd–C, MeOH, 53% yield, 85:15 anti/syn, 17% isolated yield of anti; (e) $MeSO_2Cl$, Et_3N, CH_2Cl_2; (f) NaN_3, DMF, 60 °C, 45% for steps e and f; (g) H_2, $Pd(OH)_2$, MeOH, quant; (h) phenyl 3-ethyl-5-(1-methyl-1*H*-tetrazol-5-yl)phenylcarbamate, CH_3CN, 86%; (i) TFA, CH_2Cl_2 63%; (j) formaldehyde, $NaCNBH_3$, CH_3COOH (1 drop), CH_3CN, HPLC purification, 47%.

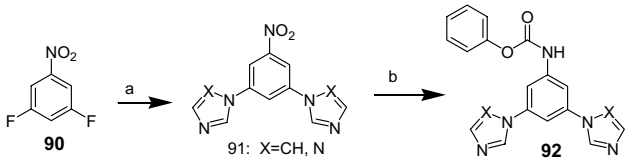

Scheme 6. Reagents and conditions: (a) imidazole/DMSO or NaH/1,2,4-triazole/DMF, 100 °C, 24 h, 60–80%; (b) i—$Pd(OH)_2$, EtOAc/MeOH, H_2; ii—2,6-lutidine, phenylchloroformate,THF/$CHCl_3$, 25 °C.

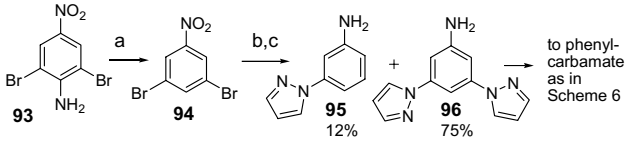

Scheme 7. Reagents and conditions: (a) i—AcOH, H_2SO_4, $NaNO_2$; ii—Cu_2O, EtOH, 80%; (b) pyrazole, CuI, K_2CO_3, NO_2Ph, Δ; (c) H_2, Pd–C, MeOH, EtOAc, 76%.

identical orientation of the benzylpiperidine and urea substituents relative to one another in both **2b** and **31** and (3) the α-methyl- (**31**) and cyclohexyl-induced (**2b**) conformation of the urea and consequently the directional positioning of the phenyl tetrazole.

Others working in the field of peptide chemistry have found that both *trans*-2-aminocyclohexylcarboxylic acid (a rigidified β-amino acid) and *syn*-α,β-disubstituted β-amino acids induce a helix when incorporated into a peptide chain.[15,16] It has been suggested[17] that the helix-inducing properties of both arise from their shared stabilized conformation, similar to what we propose in Figure 2.

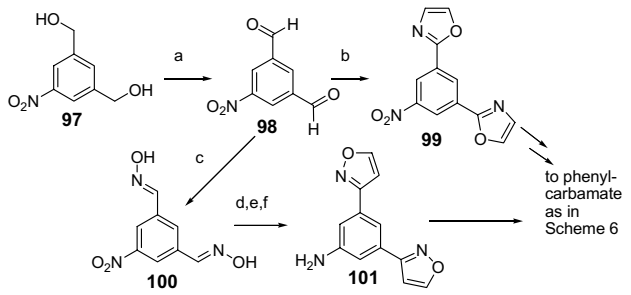

Scheme 8. Reagents and conditions: (a) DMSO, TFAA, TEA, CH_2Cl_2, −65 °C, 82%; (b) aminoacetaldehyde-dimethylacetal, P_2O_5, H_2SO_4, 77%; (c) H_2NOH–HCl, pyridine, EtOH; (d) TMS–acetylene, NaOCl, TEA, CH_2Cl_2; (e) K_2CO_3, MeOH; (f) H_2, Pd–$BaSO_4$, MeOH, EtOAc, 49%.

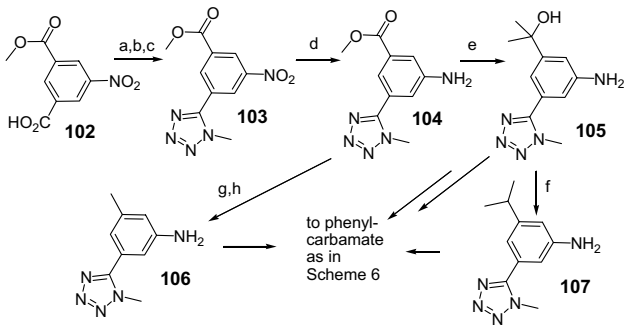

Scheme 9. Reagents and conditions: (a) ClCOCOCl, CH_2Cl_2; (b) CH_3NH_2, THF; (c) Tf_2O, NaN_3, CH_3CN, 0 °C, 72%–caution, use blast shield; (d) H_2, 10% Pd–C, MeOH, EtOAc, THF, quant; (e) MeLi, THF, 18%; (f) H_2, 10% Pd–C, MeOH, THF, concd HCl, cat., 92%; (g) LAH, THF; (h) H_2, 10% Pd–C, MeOH, concd HCl, cat., 33%.

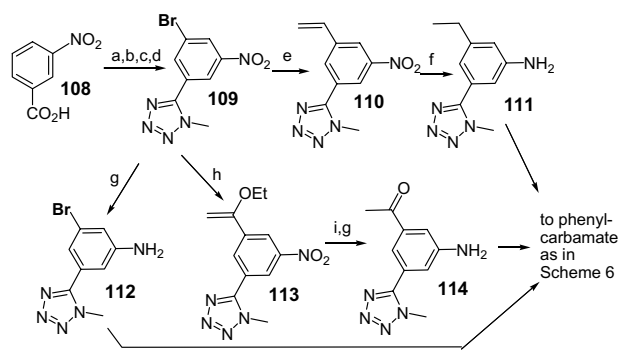

Scheme 10. Reagents and conditions: (a) NBS, TFA, H_2SO_4, 72%; (b) ClCOCOCl, CH_2Cl_2; (c) CH_3NH_2, THF, quant; (d) Tf_2O, NaN_3, CH_3CN, 0 °C, 35%–caution, use blast shield; (e) $(CH_2{=}CH)Sn(Bu)_3$, $Pd(PPh_3)_4$, THF, reflux; (f) H_2, 10% Pd–C, MeOH; (g) $SnCl_2$, EtOH, reflux, 2 h, quant; (h) $(CH_2{=}C(OEt))Sn(Bu)_3$, $Pd(PPh_3)_4$, $Pd(PPh_3)_2Cl_2$, Tol, reflux, 1 h, quant; (i) 1 N HCl, dioxane, rt, 15 min, quant.

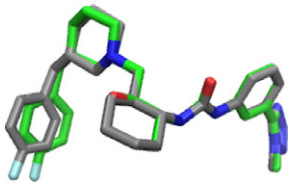

Figure 5. Overlapped ab initio minimized structures of compounds **2b** (gray) and **31** (green).

The question we now leave for the medicinal chemist is whether the 16,000 compounds in the literature containing the *syn*-(1,3-diamino-2-hydroxy-1-methyl)propyl substructure present in **31** can be converted into appropriately substituted cyclohexane-containing molecules with retention of biological activity.

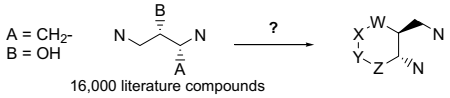

Acknowledgments

We thank the members of the Separations Group, Al Mical, Dauh-Rurng Wu, and Kathy Rathgeb for purifying the mother liquors of **75** during the kilo-scale synthesis of **31**. We thank Srinivas Tummala, Ehrlic Lo, and Steve Wang of the Process Research Dept. for performing the kilo-scale hydrogenation of **74**. We also thank the members of the Chemical Synthesis Group, Chris Teleha, Gary Cain, Sergei Bobkov, Jan Hytrek, Chris Tabaka, and George Emmett, for the large-scale preparation of **60** employed in the kilo-scale synthesis of **31**. We also thank Sarah Traeger for NMR studies on **31** and **2b**.

Supplementary data

Supplementary data associated with this article can be found, in the online version, at doi:10.1016/j.bmcl.2007.11.067.

References and notes

1. For reviews on eotaxin, CCR3 receptors, and eosinophils in asthma, see (a) Corrigan, C. *Curr. Opin. Investig. Drugs* **2000**, *1*, 321; Strek, M. E.; Leff, A. R. In *Asthma*; Barnes, P. J., Grunstein, M. M., Leff, A. R., Woolcock, A. J., Eds.; Lippincott-Raven: Philadelphia, 1997; Owen, C. *Pulm. Pharm. Ther.* **2001**, *14*, 193; Erin, E. M.; Williams, T. J.; Barnes, P. J.; Hansel, T. T. *Curr. Drug Targets-Inflamm. Allergy* **2002**, *1*, 201; Bertrand, C. P.; Ponath, P. D. *Exp. Opin. Invest. Drugs* **2000**, *9*, 43; Elsner, J.; Escher, S. E.; Forssmann, U. *Allergy* **2004**, *59*, 1243; (b) For other small molecule CCR3 antagonists in the literature, see Ref. 3 and citations therein.
2. Varnes, J. G.; Gardner, D. S.; Santella, J. B.; Duncia, J. V.; Estrella, M.; Watson, P. S.; Clark, C. M.; Ko, S. S.; Welch, P.; Covington, M.; Stowell, N.; Wadman, E.; Davies, P.; Solomon, K.; Newton, R. C.; Trainor, G. L.; Decicco, C. P.; Wacker, D. *Bioorg. Med. Chem. Lett.* **2004**, *14*, 1645.
3. De Lucca, G. V.; Kim, U.-T.; Vargo, B. J.; Duncia, J. V.; Santella, J. B., III; Gardner, D. S.; Zheng, C.; Liauw, A.; Wang, Z.; Emmett, G.; Wacker, D. A.; Welch, P. K.; Covington, M.; Stowell, N. C.; Wadman, E. A.; Das, A. M.; Davies, P.; Yeleswaram, S.; Graden, D. M.; Solomon, K. A.; Newton, R. C.; Trainor, G. L.; Decicco, C. P.; Ko, S. S. *J. Med. Chem.* **2005**, *48*, 2194.

4. For a description of the CCR3 binding, the human eosinophil chemotaxis, and the intracellular Ca^{2+} flux assays, see Ref. 3.
5. For a discussion of the disconnect between the binding and chemotaxis IC_{50} values, see Ref. 3.
6. In vivo clearance was projected from in vitro oxidative metabolism in human liver microsomes using the $t_{1/2}$ method, as described by Obach, R. S.; Baxter, J. G.; Liston, T. E.; Silber, B. M.; Jones, B. C.; MacIntyre, F.; Rance, D. J.; Wastall, P. *J. Pharm. Exp. Ther.* **1997**, *283*, 46.
7. The binding assay was carried out using ^{125}I-labeled eotaxin and CHO cells stably transfected with a gene encoding a chimeric receptor, consisting of the intracellular domain of human CCR2 with the extracellular and transmembrane domains of human CCR3. This variation was found to give results nearly identical to those obtained using the native CCR3 receptor. Details may be found in US 2005/0123972, published on June 9, 2005.
8. (a) The starting geometry for model 1 was the lowest energy conformation found in 1000 steps of Monte-Carlo conformational searching. Models 2–4 were derived from the low energy model 1 structure via deletion of the appropriate atoms and minimization to the closest local minimum. Intermediate geometries were calculated by dihedral driving where the dihedral is constrained to the indicated angle and the remainder of the molecule allowed to relax. Final energies were calculated by a single point ab initio calculation at the B3LYP/6-31G** level of theory with a water solvation model. The resulting low energy conformation for each model was then used as the starting structure for torsion 2. The energetics of torsion 2 were evaluated as above except torsion 1 was constrained to its starting value. The Monte-Carlo and dihedral drive calculations were conducted with the conformational search and dihedral drive modules of MacroModel[8b] using the MMFF94s force field in water. Ab initio energies were calculated using Jaguar.[8c]; (b) MacroModel, version 9.1, Schrödinger LLC, New York, NY, 2005.; (c) Jaguar, version 6.5, Schrödinger LLC, New York, NY, 2005.
9. Hoffmann, R. W. *Chem. Rev.* **1989**, *89*, 1841.
10. (a) Bunnage, M. E.; Chernega, A. N.; Davies, S. G.; Goodwin, C. J. *J. Chem. Soc. Perkin Trans. 1* **1994**, 2373; (b) Davis, F. A.; Weismiller, M. C.; Murphy, C. K.; Thimma Reddy, R.; Chen, B.-C. *J. Org. Chem.* **1992**, *57*, 7274.
11. Beaulieu, P. L.; Wernic, D. *J. Org. Chem.* **1996**, *61*, 3635.
12. Burke, A. A.; Davies, S. G.; Hedgecock, C. J. R. *Synlett* **1996**, 621.
13. Davies, S. G.; Walters, I. A. S. *J. Chem. Soc. Perkin Trans. 1* **1994**, 1129.
14. Ulrich, P. *J. Med. Chem.* **1984**, *27*, 35.
15. Lee, M.-r.; Raguse, T. L.; Schinnerl, M.; Pomerantz, W. C.; Wang, X.; Wipf, P.; Gellman, S. H. *Org. Lett.* **2007**, *9*, 1801, and references therein.
16. Seebach, D.; Abele, S.; Gademann, K.; Guichard, G.; Hintermann, T.; Jaun, B.; Matthews, J. L.; Schreiber, J. V. *Helv. Chim. Acta* **1998**, *81*, 932, and references therein.
17. Gung, B. W.; Zhu, Z. *J. Org. Chem.* **1997**, *62*, 6100.